Electronic Supporting information

Highly Luminescent Copper(I) Halide Complexes Chelated with a Tetradentate Ligand (PNNP): Synthesis, Structure, Photophysical Properties and Theoretical Studies

Ji-Hui Jia,[a,c] Xu-Lin Chen,*[a,b] Jian-Zhen Liao,[a] Dong Liang,[b] Ming-Xue Yang,[a,c] Rongmin Yu,[a] and Can-Zhong Lu*[a,b]

[a]*Key Laboratory of Design and Assembly of Functional Nanostructures, and Fujian Key Laboratory of Nanomaterials, Fujian Institute of Research on the Structure of Matter, Chinese Academy of Sciences, Fuzhou, Fujian 350002, China*

[b]*Xiamen Institute of Rare-earth Materials, Haixi Institutes, Chinese Academy of Sciences, Xiamen 361021, China*

[c]*University of Chinese Academy of Sciences, Beijing, 100049, China.*

1. Crystal Structure Determination

Table S1. Selected crystallographic data of the complexes **1** and **2**.

Compound reference	1	2
Chemical formula	$C_{48}H_{36}Br_2Cu_2N_4P_2$	$C_{48}H_{36}Cu_2I_2N_4P_2$
Formula Mass	1017.65	1111.63
Crystal system	triclinic	triclinic
a/Å	12.0271(5)	12.2493(4)
b/Å	13.1399(8)	13.0962(6)
c/Å	17.0209(8)	17.0110(7)
α/°	109.974(5)	107.746(4)
β/°	92.594(4)	92.742(3)
γ/°	113.357(5)	114.186(4)
Unit cell volume/Å^3	2269.5(2)	2323.58(16)
Temperature/K	100(2)	100(2)
Space group	P-1	P-1
No. of formula units per unit cell, Z	2	2
No. of reflections measured	15788	16036
No. of independent reflections	8945	9173
R_{int}	0.0318	0.0293
Final R_1values ($I > 2\sigma(I)$)	0.0375	0.0301
Final $wR(F^2)$ values ($I > 2\sigma(I)$)	0.0952	0.982
Final R_1values (all data)	0.0490	0.0332
Final $wR(F^2)$ values (all data)	0.1014	0.0827
Goodness of fit on F^2	1.044	0.982
CCDC reference numbers	1853178	1853179

[a]$R_1 = \sum ||F_o| - |F_c|| / \sum |F_o|$. [b]$wR_2 = [\sum w(F_o^2 - F_c^2)^2 / \sum w(F_o^2)]^{1/2}$

Table S2. Selected bond distances (Å) and angles (º) of the complexes **1** and **2**.

Compound		1	2
Distances(Å)	Cu1-X1	2.51	2.63
	Cu1-N1	2.16	2.16
	Cu1-P1	2.21	2.24
	Cu1-X2	2.47	2.66
	Cu1-Cu2	3.04	2.96
Angles(℃)	P1-Cu1-N1	91.95	90.62
	P1-Cu1- X2	120.95	115.39
	P1-Cu1-X1	118.18	117.05
	X1-Cu1-X2	103.71	110.51
	X1-Cu1-N1	103.02	118.21
	X2-Cu1-N1	118.05	103.17

Scheme 1. Synthetic route of the ligand.

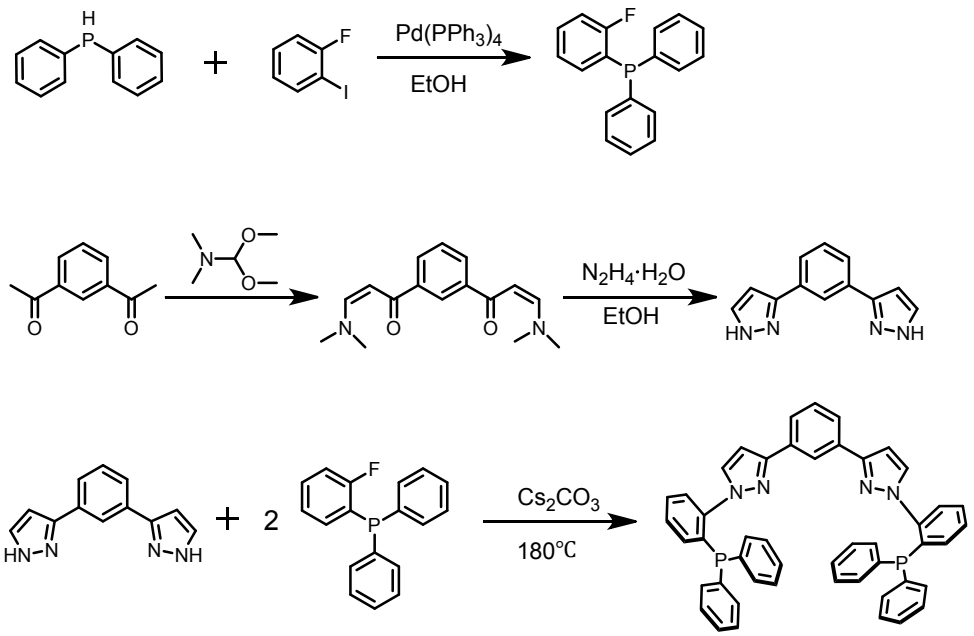

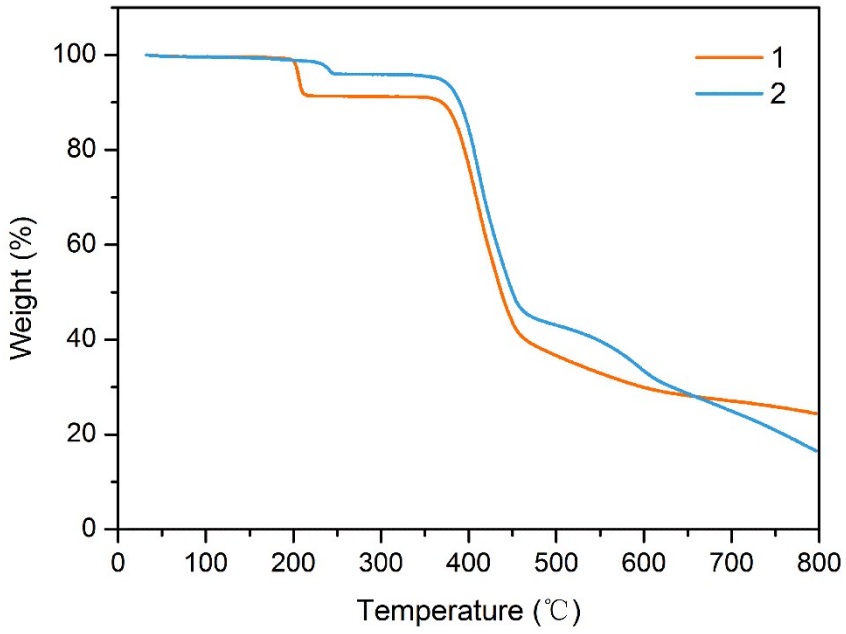

Figure S1 TGA-plots for complexes **1** and **2**.

2. Theoretical Studies

Table S3 Composition of HOMO, HOMO-1, LUMO, and LUMO+1 of complexes **1**-**2** in the optimized S_0 structure.

		Cu	X	P	C,N,H
Compound1	HOMO-6	67.073502%	13.016883%	5.415852%	14.493763%
	HOMO-5	64.053482%	22.542768%	0.389114%	13.014636%
	HOMO-4	75.187452%	7.107629%	2.887000%	14.817919%
	HOMO-3	42.513077%	52.606468%	0.387677%	4.492778%
	HOMO-2	52.849406%	27.892934%	7.107275%	12.150385%
	HOMO-1	54.114584%	28.768855%	6.109894%	11.006667%
	HOMO	53.150280%	20.087406%	15.792438%	10.969877%
	LUMO	1.551162%	0.913887%	5.191978%	92.342973%
	LUMO+1	3.725925%	0.425068%	4.323489%	91.525518%
	LUMO+2	8.908469%	0.087289%	5.136377%	85.867865%
	LUMO+3	1.066420%	0.074555%	10.728958%	88.130067%
	LUMO+4	3.663999%	0.029245%	11.961106%	84.345650%
	LUMO+5	1.836927%	0.210368%	5.042766%	92.909939%
	LUMO+6	21.056377%	0.076414%	2.576834%	76.290375%
Compound2	HOMO-6	51.814554%	18.066024%	10.272232%	19.847190%
	HOMO-5	53.021560%	31.014925%	1.483943%	14.479572%
	HOMO-4	66.467396%	14.272471%	3.635088%	15.625045%
	HOMO-3	28.729365%	67.013672%	0.285326%	3.971637%
	HOMO-2	42.180593%	39.134520%	6.907102%	11.777785%
	HOMO-1	46.044242%	40.419744%	4.521937%	9.015899%
	HOMO	45.992967%	28.792098%	15.059474%	10.155461%
	LUMO	4.878275%	0.573204%	4.211374%	90.337147%
	LUMO+1	1.683849%	1.249788%	5.123323%	91.943040%
	LUMO+2	9.161551%	0.112161%	5.719065%	85.007223%
	LUMO+3	1.437793%	0.075148%	11.991131%	86.495928%
	LUMO+4	3.249861%	0.052653%	11.472226%	85.225260%
	LUMO+5	1.910525%	0.319175%	3.830257%	93.940043%
	LUMO+6	24.202168%	0.116710%	2.792612%	72.888510%

Table S4 Compositions of hole and electron in the S_1 state of **1** and **2** in the optimized S_0 structure.

		Cu	X	P	C,N,H
Compound1	Hole	54.724997%	17.898719%	16.141038%	11.235246%
	electron	2.288220%	1.358306%	5.654734%	90.698740%
	difference	52.44%	16.54%	10.47%	-79.46%
Compund2	Hole	47.832405%	26.569939%	15.368771%	10.228884%
	electron	2.457454%	1.781833%	5.459608%	90.301105%
	difference	45.37%	24.79%	9.91%	-80.07%

Table S5 Compositions of hole and electron in the T_1 state of **1** and **2** in the optimized S_0 structure.

		Cu	X	P	C,N,H
Compound1	Hole	50.975823%	15.076068%	18.148691%	15.799418%
	electron	2.289848%	1.420924%	7.940988%	88.348240%
	difference	48.685975%	13.655144%	10.207703%	-72.55%
Compund2	Hole	45.437657%	23.047326%	17.434178%	14.080840%
	electron	2.529659%	1.976107%	7.454214%	88.040021%
	difference	42.907998%	21.071219%	9.979934%	-73.96%

Table S6 Calculated energy levels, oscillator strengths (*f*), and orbital transition analyses for selected lower-lying transitions for complexes **1** and **2**

	states	λ_{cal} (nm)	*f*	assignments	MLCT	XLCT	ILCT
1	S_1	413.03	0.0026	HOMO→LUMO (89%)	52.44%	16.54%	10.47%
	S_2	410.60	0.0119	HOMO→LUMO+1 (87%)			
	S_3	381.86	0.0016	HOMO-1→LUMO (83%)			
	T_1	429.20	0.0	HOMO→LUMO (74%) HOMO-1→LUMO+1 (11%)	48.69%	13.66%	10.21%
2	S_1	415.49	0.0022	HOMO→LUMO+1 (93%)	45.37%	24.79%	9.91%
	S_2	413.83	0.0106	HOMO→LUMO (94%)			
	S_3	384.52	0.003	HOMO-1→LUMO (92%)			
	T_1	428.65	0.0	HOMO→LUMO+1 (80%)	42.91%	21.07%	9.98%

Table S7 Compositions of hole and electron in the S_1 state of **1** and **2** in the optimized S_1 structure.

		Cu	X	P	C,N,H
Compound1	Hole	49.348000%	11.506052%	18.511014%	20.634934%
	electron	2.245564%	0.670512%	3.543305%	93.540619%
	difference	47.10%	10.84%	14.97%	-72.91%
Compund2	Hole	45.286435%	17.160418%	17.986002%	19.567145%
	electron	2.419814%	0.859895%	3.413330%	93.306961%
	difference	42.87%	16.30%	14.57%	-73.74%

Table S8 Compositions of hole and electron in the T_1 state of **1** and **2** in the optimized T_1 structure.

		Cu	X	P	C,N,H
Compound1	Hole	45.449827%	10.329748%	20.336456%	23.883969%
	electron	2.359396%	0.857278%	7.200250%	89.583076%
	difference	43.09%	9.47%	13.14%	-65.70%
Compund2	Hole	41.249002%	14.291310%	20.526102%	23.933586%
	electron	2.438149%	1.093314%	7.465256%	89.003280%
	difference	38.81%	13.20%	13.06%	-65.07%

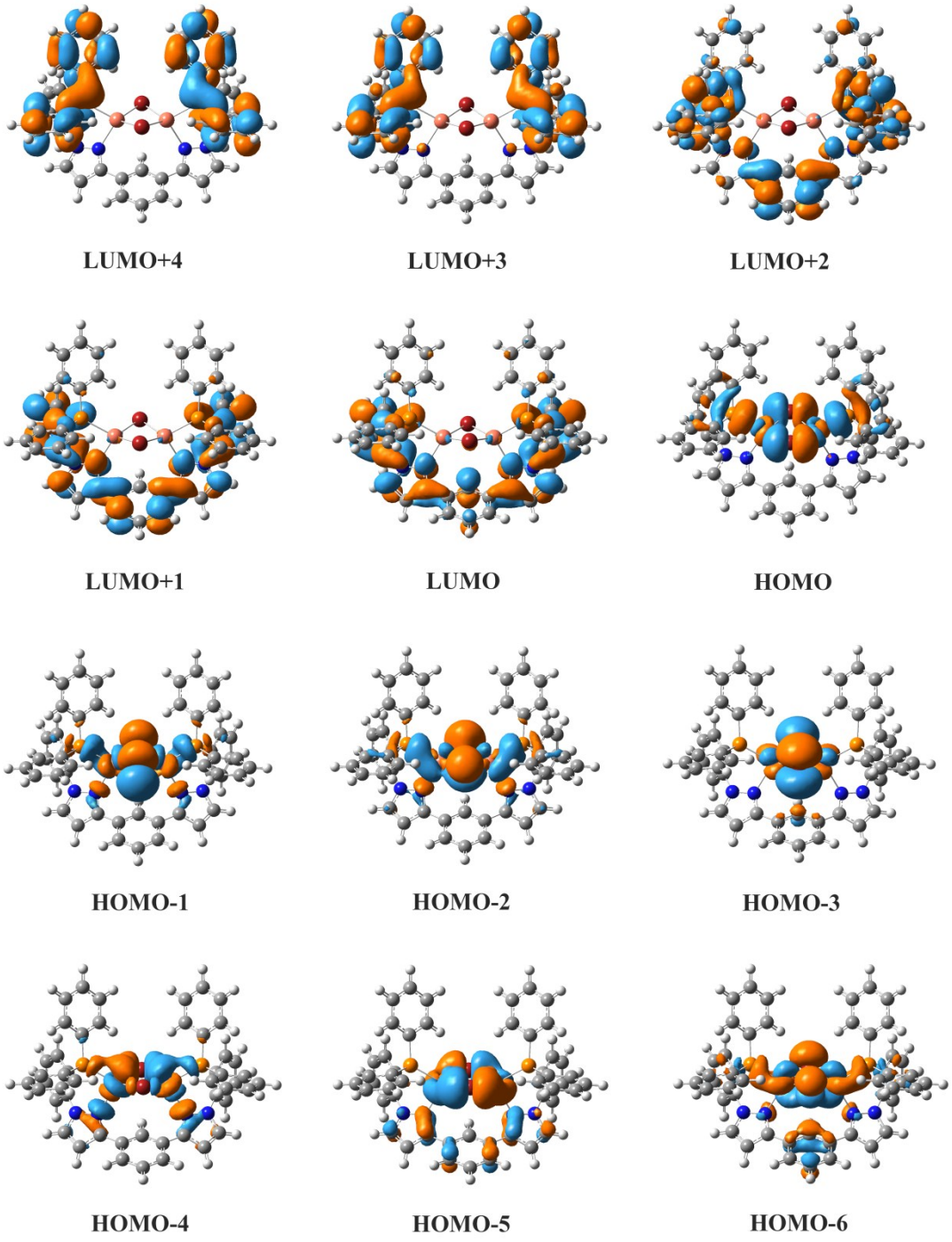

Figure S2 Frontier orbitals from HOMO-6 to LUMO+4 of complex **1** in the optimized S_0 structure

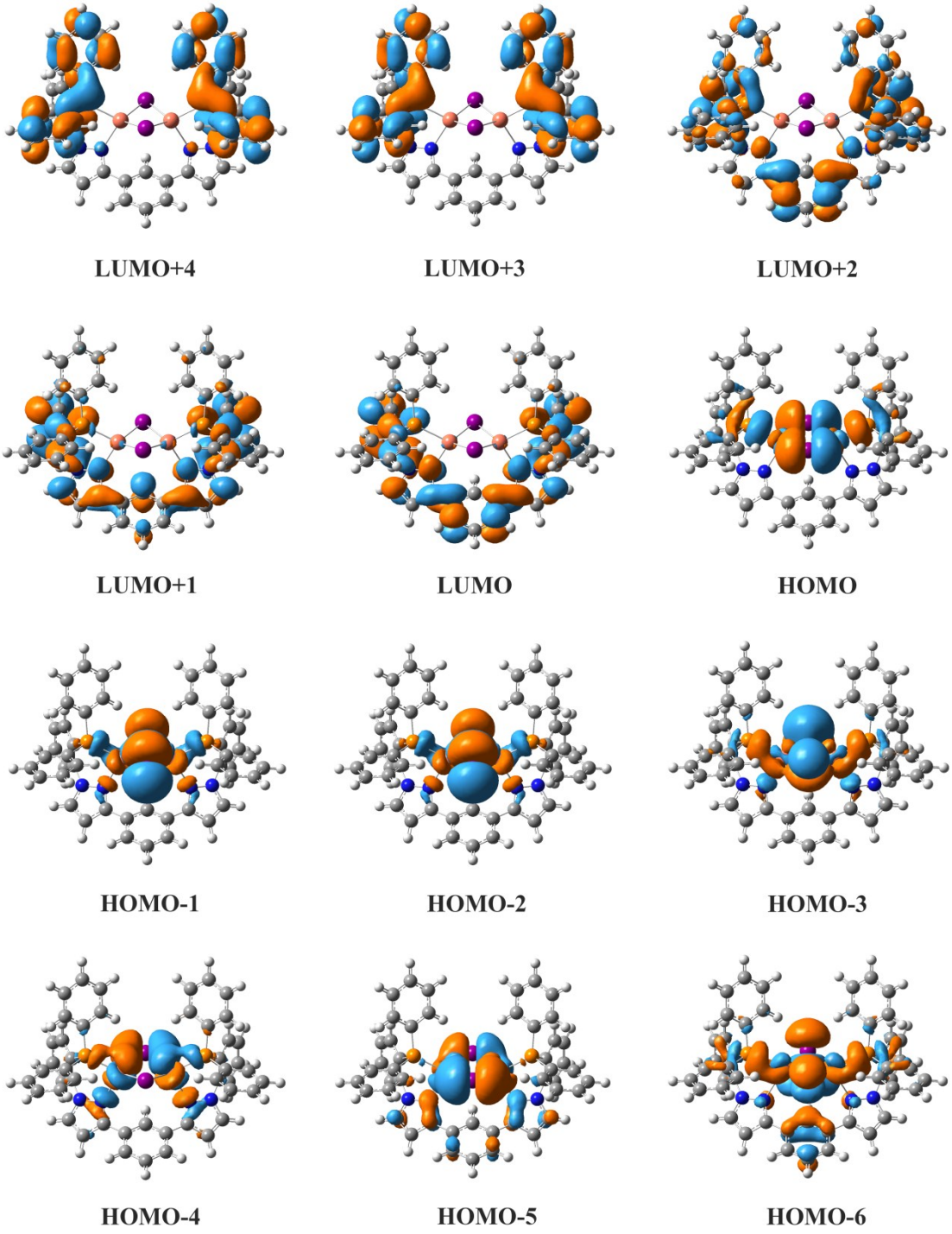

Figure S3 Frontier orbitals from HOMO-6 to LUMO+4 of complex **2** in the optimized S_0 structure.

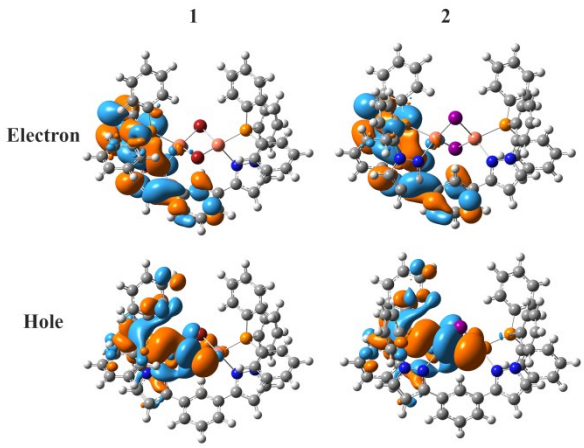

Figure S4 Natural transition orbital pairs of the S_1 state for complexes **1** and **2** in the optimized S_1 structure.

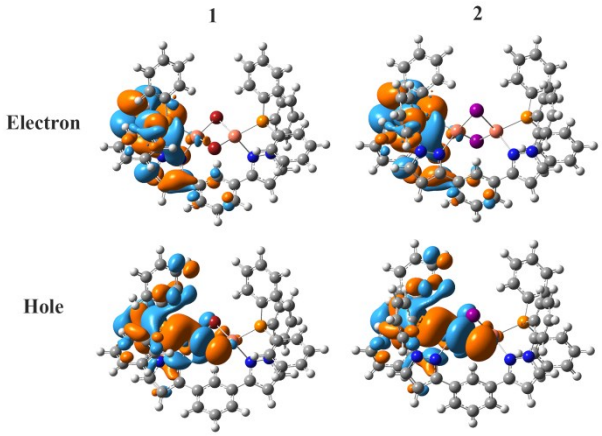

Figure S5 Natural transition orbital pairs of the T_1 state for complexes **1** and **2** in the optimized T_1 structure.

In order to evaluated the temperature-dependent relative contributions of TADF and phosphorescence in the overall emission, we estimated the ratio of the individual emission intensity originating from S_1 and T_1, i.e., $I(S_1)$ and $I(T_1)$, to the total emission intensity I_{tot}, in dependence of temperature. The emission intensity is proportional to the population of the individual state N and to the corresponding radiative rate constant k_r, so we can obtain:

$$I(S_1) = \alpha N(S_1) k_r(S_1) = \alpha N(S_1) \emptyset_{PL}(S_1) \tau(S_1)^{-1} (S1)$$

$$I(T_1) = \alpha N(T_1) k_r(T_1) = \alpha N(T_1) \emptyset_{PL}(T_1) \tau(T_1)^{-1} (S2)$$

Herein, α is the proportionality constant that is same in both the equations. Assuming that the populations of both states follow a Boltzmann distribution (fast equilibration), the relative intensities can be expressed as follows:

$$\frac{I(T_1)}{I_{tot}} = \frac{I(T_1)}{I(S_1) + I(T_1)} = \left[1 + \frac{I(S_1)}{I(T_1)}\right]^{-1} = \left[1 + \frac{\alpha N(S_1) \emptyset_{PL}(S_1) \tau(S_1)^{-1}}{\alpha N(T_1) \emptyset_{PL}(T_1) \tau(S_1)^{-1}}\right]^{-1}$$
$$= \left[1 + \frac{N(S_1) \emptyset_{PL}(S_1) \tau(T_1)}{N(T_1) \emptyset_{PL}(T_1) \tau(S_1)}\right]^{-1} = \left[1 + \frac{\emptyset_{PL}(S_1) \tau(T_1) g(S_1)}{\emptyset_{PL}(T_1) \tau(S_1) g(T_1)} \exp\left(-\frac{\Delta E_{ST}}{K_B T}\right)\right]^{-1} \# \quad (S3)$$

$$\frac{I(S_1)}{I_{tot}} = 1 - \frac{I(T_1)}{I_{tot}} = 1 - \left[1 + \frac{\emptyset_{PL}(S_1) \tau(T_1) g(S_1)}{\emptyset_{PL}(T_1) \tau(S_1) g(T_1)} \exp\left(-\frac{\Delta E_{ST}}{K_B T}\right)\right]^{-1} \# (S4)$$

where $g(S_1) = 1$ and $g(T_1) = 3$ are the degeneracy factors for the singlet and the triplet states, respectively. The splitting of the T_1 state, that is, the zero-field splitting (ZFS), is distinct in organo-transition-metal compounds due to the high metal participation and large spin-orbit coupling. So, we take into account the degeneracy factors for the singlet and the triplet states ($g(S_1) = 1$ and $g(T_1) = 3$) in evaluating the populations of the two states (Boltzmann distribution).

The plots shown in Figure 6c and Figure 6d can be obtained using eq S3 and eq S4, in which the parameters have been determined by eq 2 (see Figure 6a and Figure 6b). As a result, the relative contributions of TADF and phosphorescence are depicted visually in Figure 6c and Figure 6d.

NMR Experiments

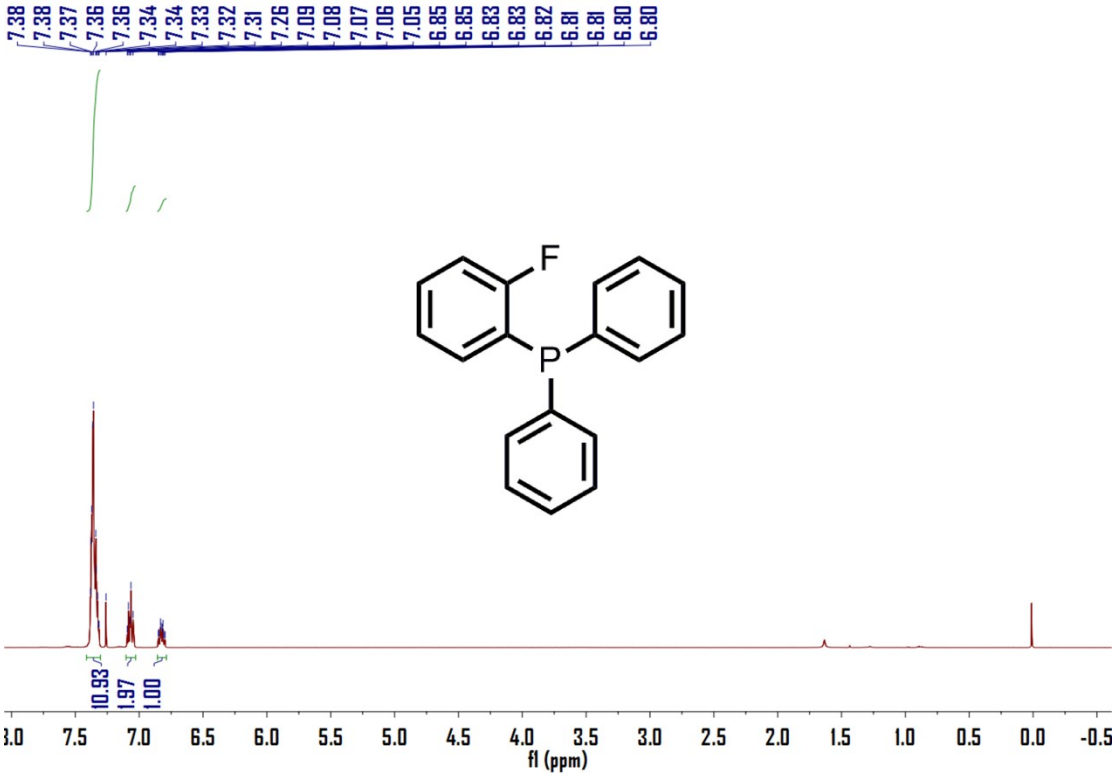

Figure S6 ^{1}H NMR spectrum of (2-fluorophenyl)diphenylphosphine in $CDCl_3$.

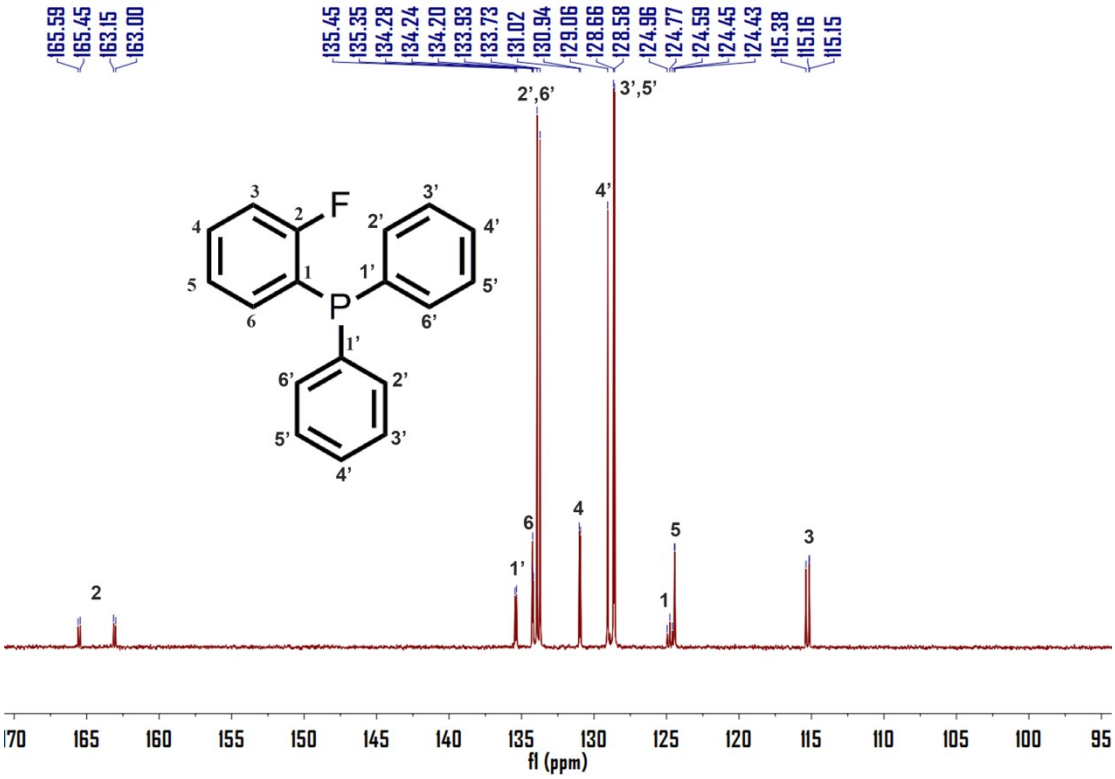

Figure S7 ^{13}C NMR spectrum of (2-fluorophenyl)diphenylphosphine in $CDCl_3$.

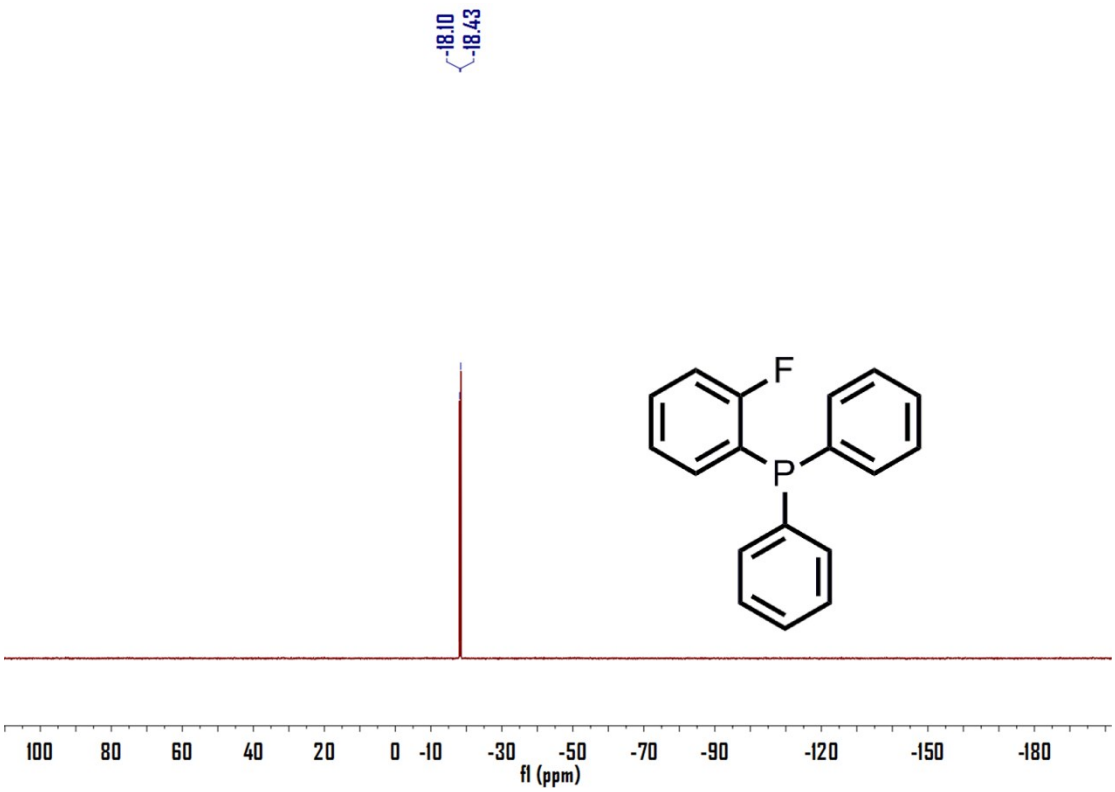

Figure S8 ^{31}P NMR spectrum of (2-fluorophenyl)diphenylphosphine in $CDCl_3$.

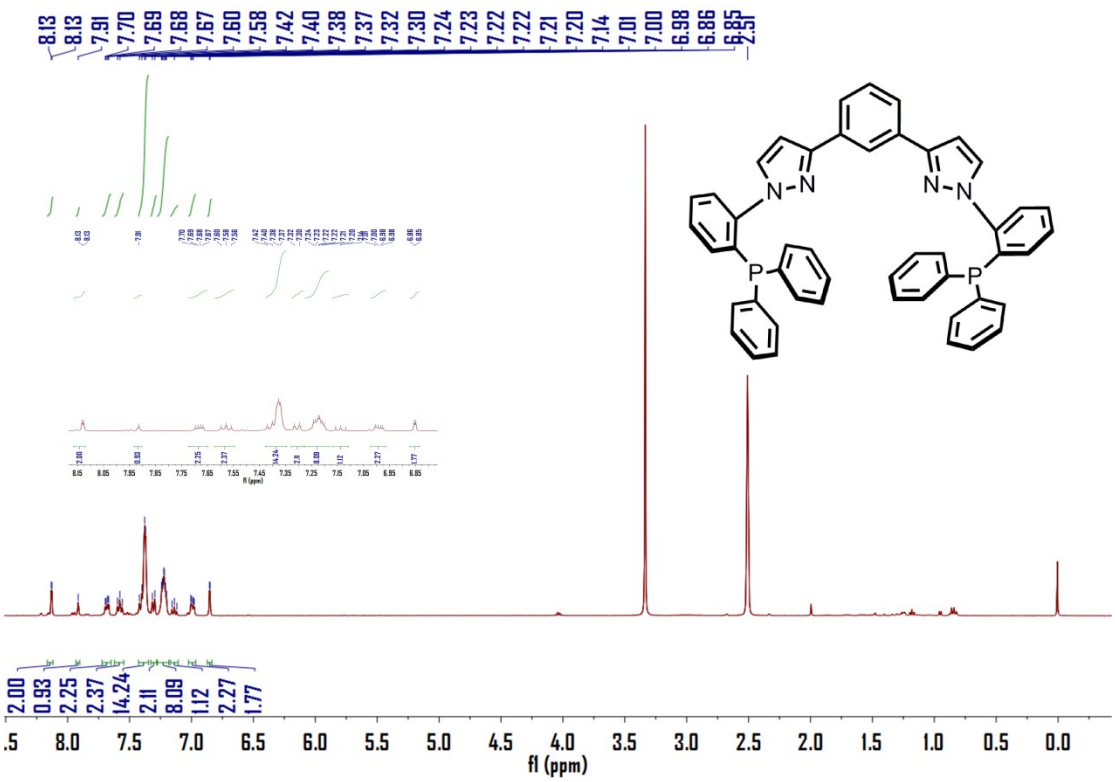

Figure S9 ^{1}H NMR spectrum of PNNP in DMSO-d_6.

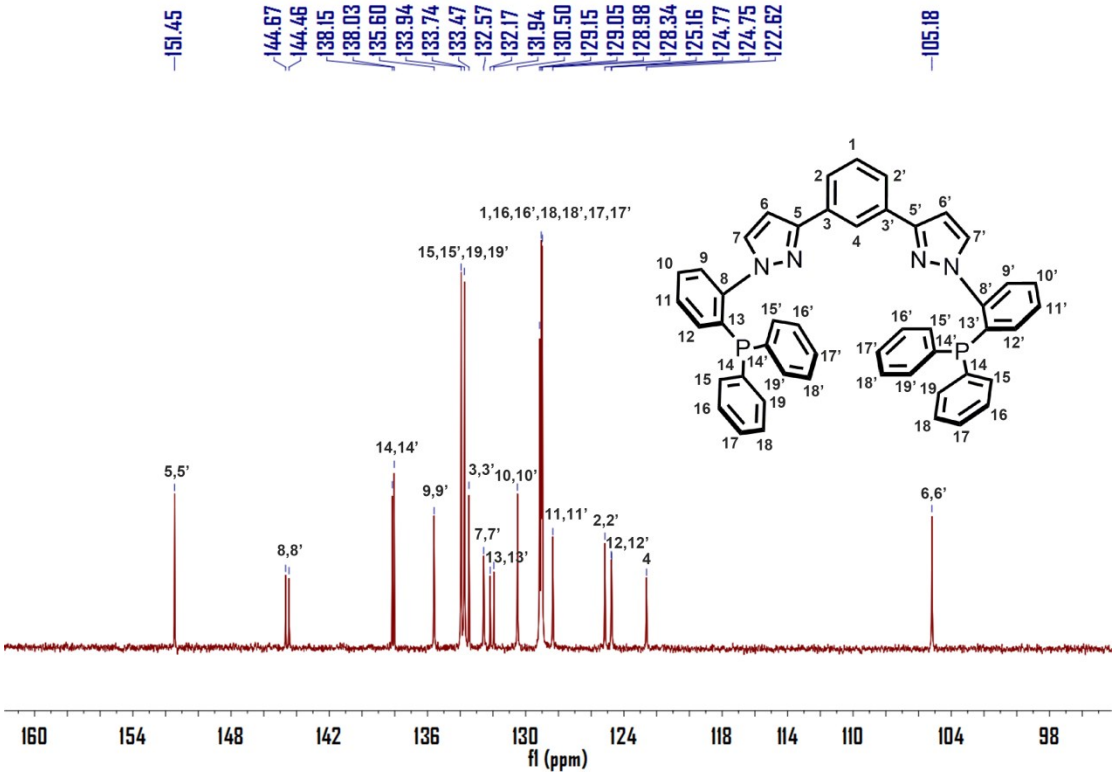

Figure S10 ^{13}C NMR spectrum of PNNP in DMSO-d_6.

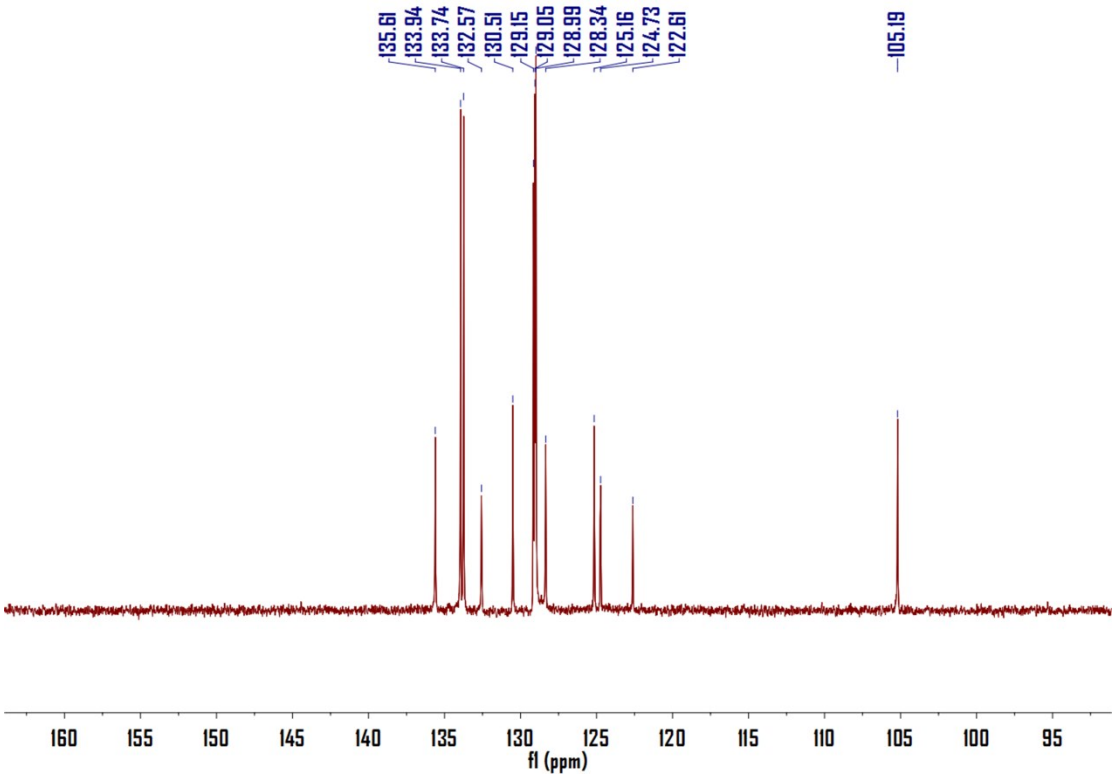

Figure S11 DEPT(135°) NMR spectrum of PNNP in DMSO-d_6.

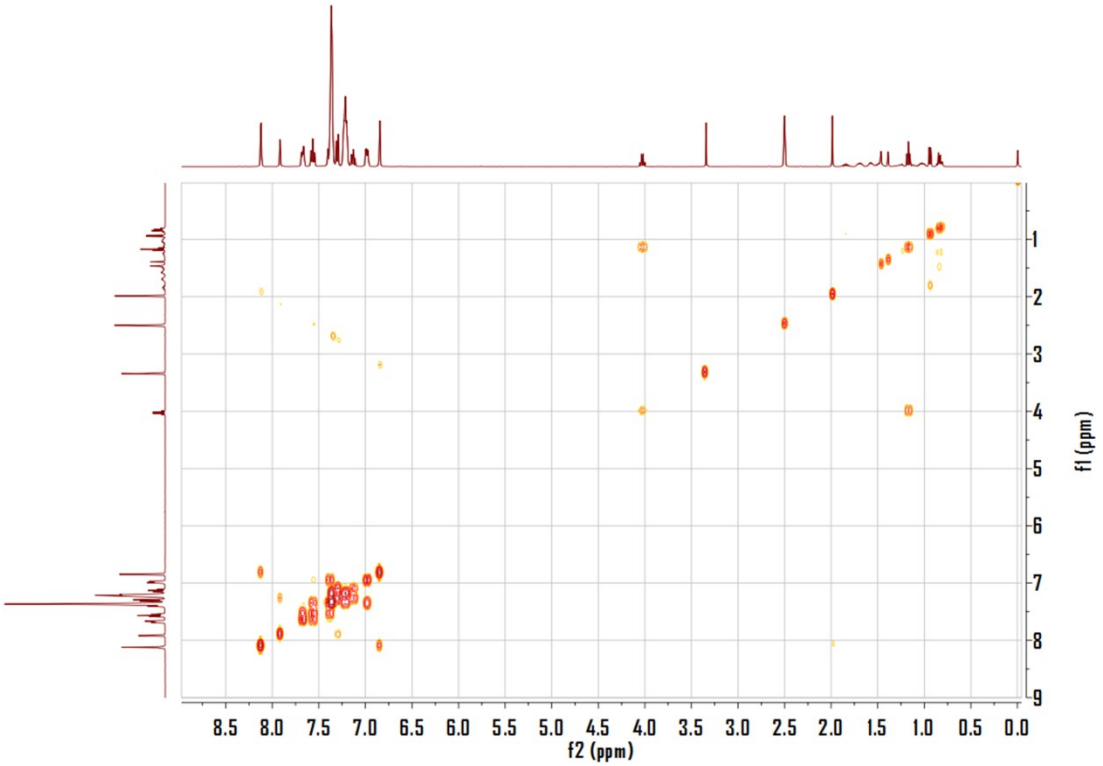

Figure S12 ^{1}H-^{1}H COSY NMR spectrum of PNNP in DMSO-d_6.

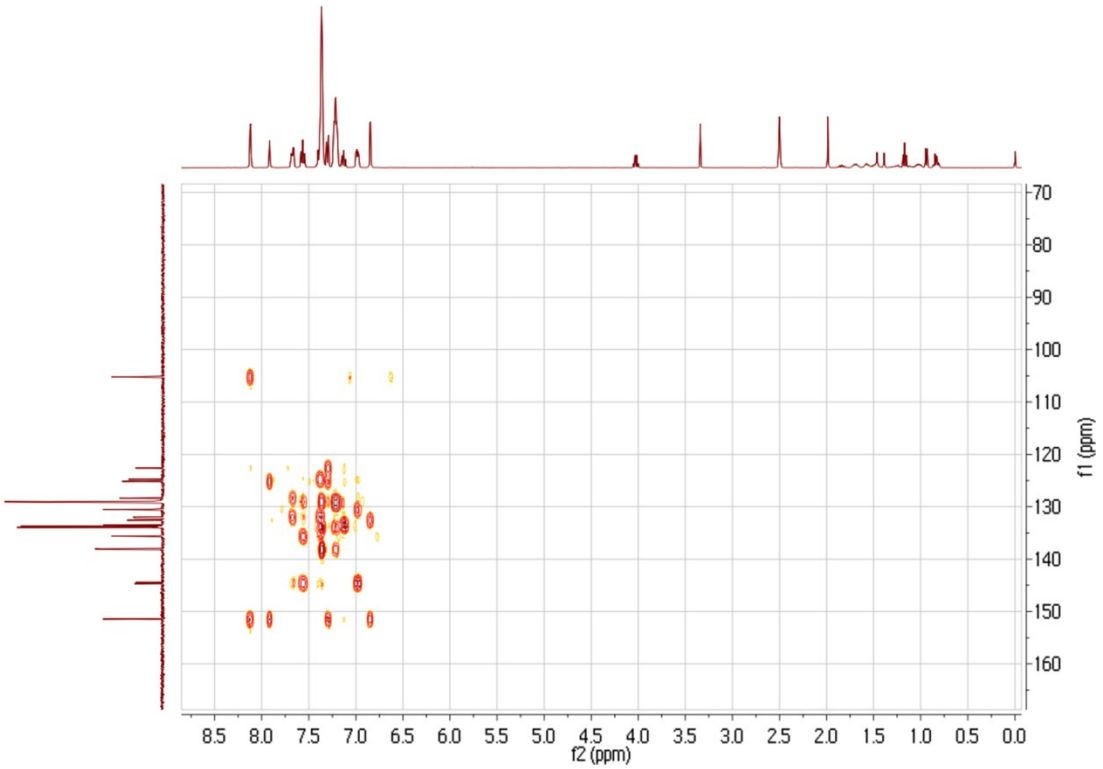

Figure S13 ^{1}H-^{13}C HMBC NMR spectrum of PNNP in DMSO-D_6.

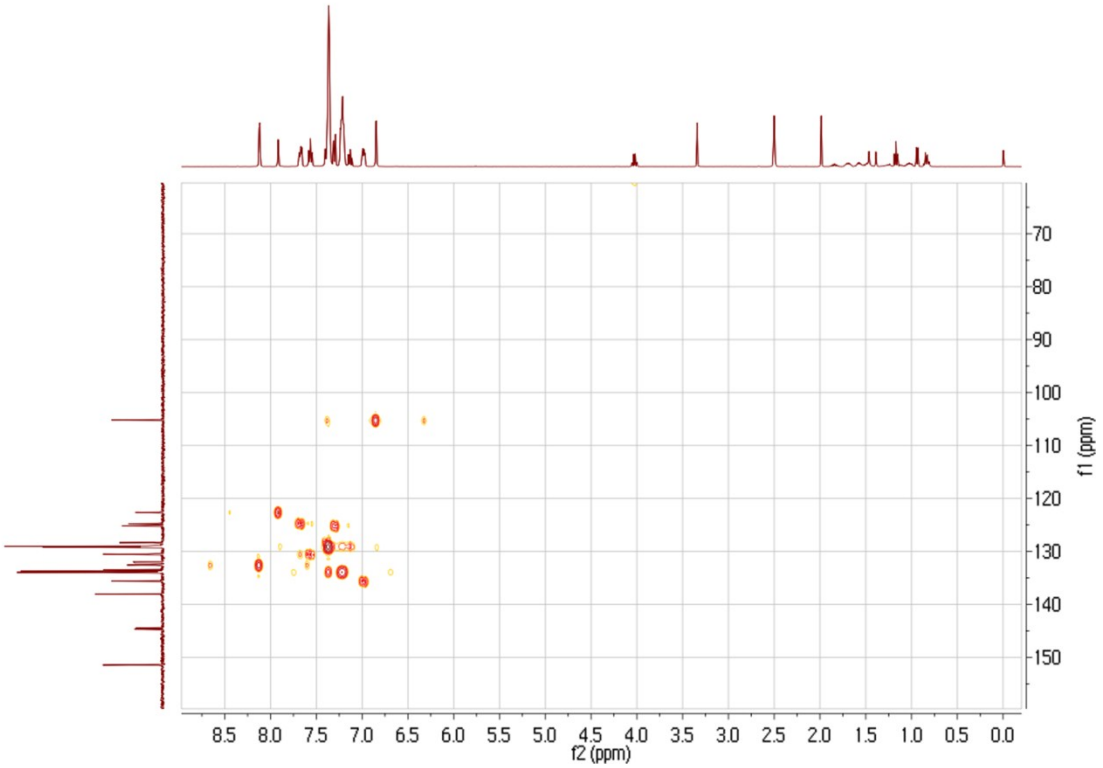

Figure S14 ^{1}H-^{13}C HMQC NMR spectrum of PNNP in DMSO-D_6

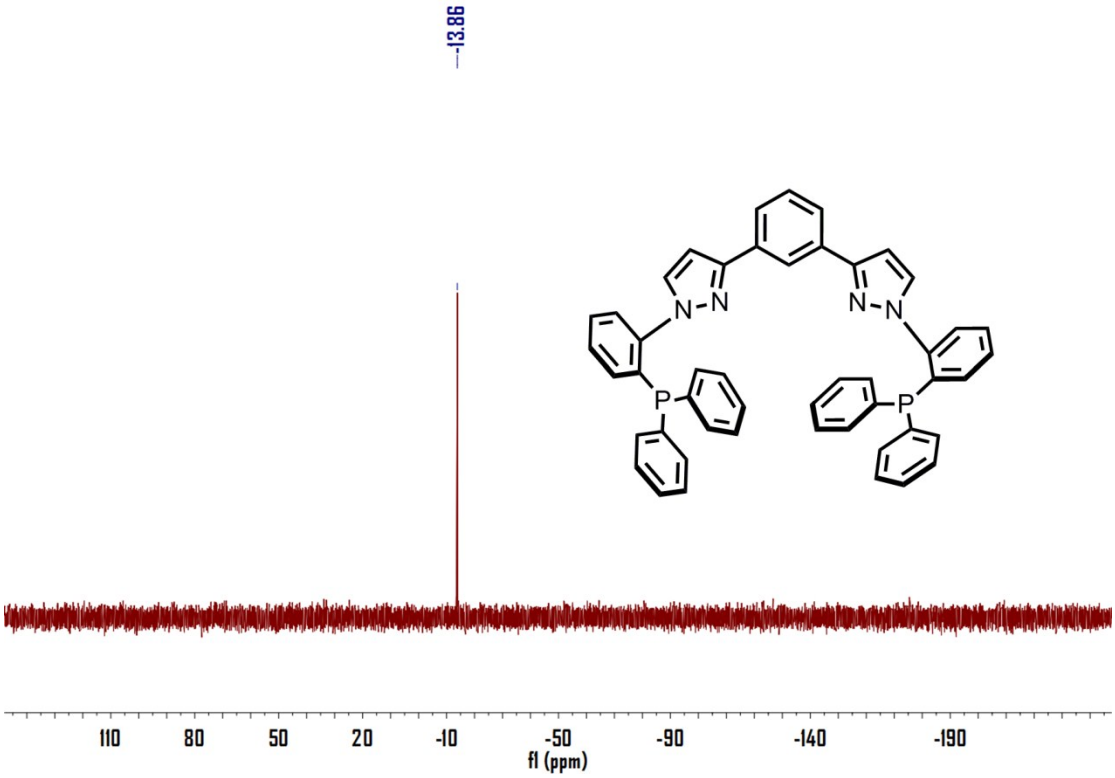

Figure S15 ^{31}P NMR spectrum of PNNP in DMSO-d_6.

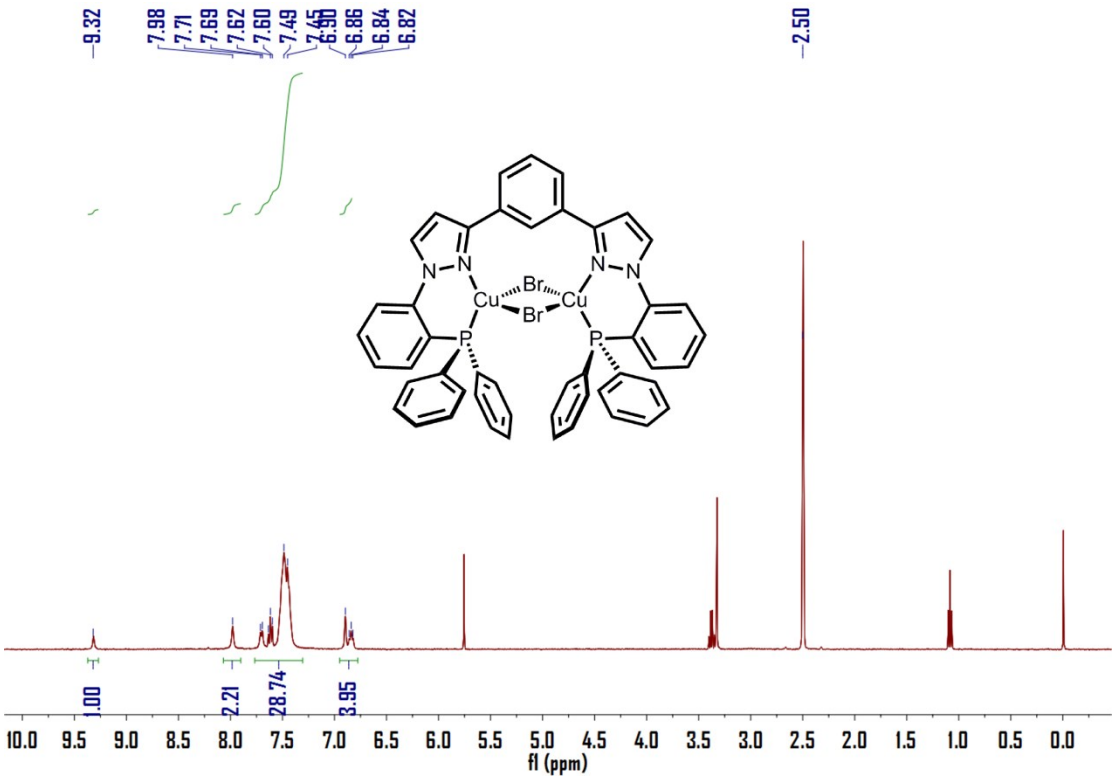

Figure S16 ^{1}H NMR spectrum of complex **1** in DMSO-d_6.

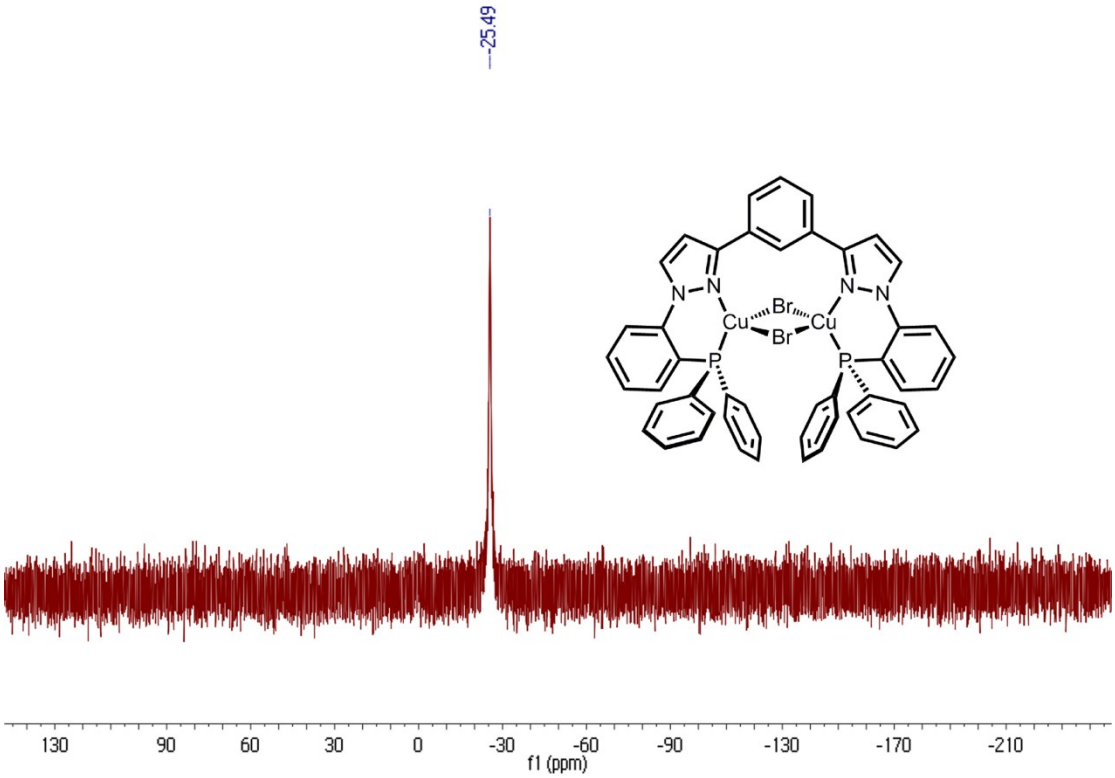

Figure S17 ^{31}P NMR spectrum of complex **1** in DMSO-d_6.

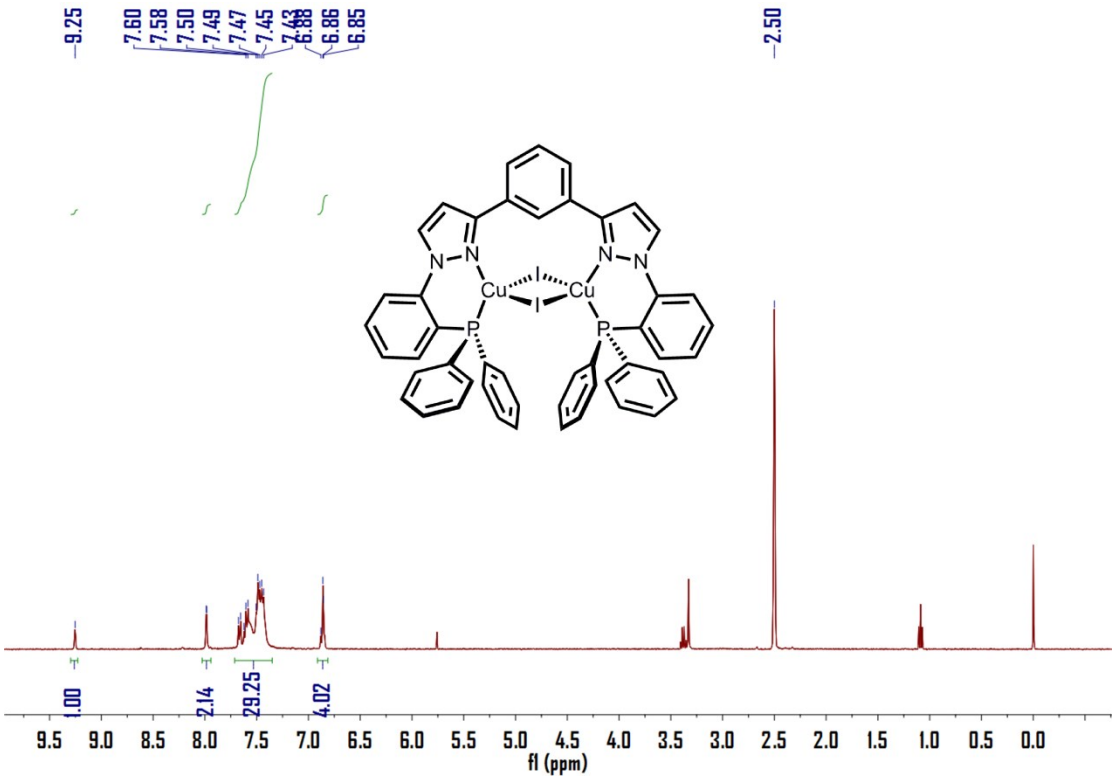

Figure S18 ^{1}H NMR spectrum of complex **2** in DMSO-d_6.

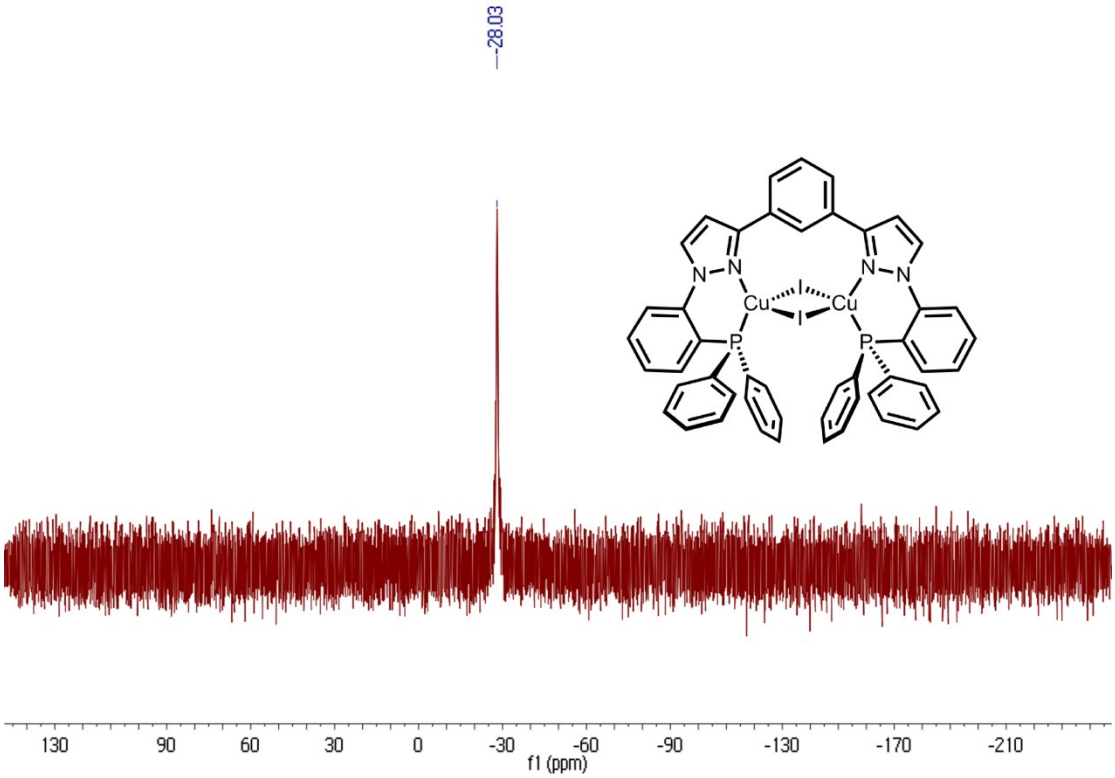

Figure S19 ^{31}P NMR spectrum of complex **2** in DMSO-d_6.

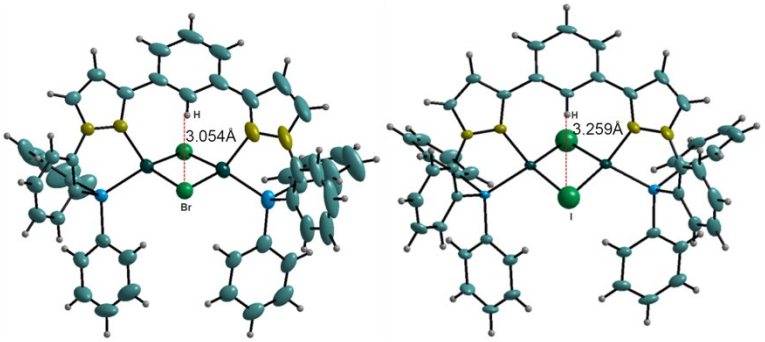

Figure S20 The intramolecular hydrogen bonds of complexes **1** and **2.**